ACS OMEGA

Open Access

http://pubs.acs.org/journal/acsodf

Article

Discovery of New Cyclic Lipodepsipeptide Orfamide N via Partnership with Middle School Students from the Boys and Girls Club

Jin Yi Tan, Mario Augustinović, Ashraf M. Omar, Vitor B. Lourenzon, Nyssa Krull, Xochitl Lopez, Manead Khin, Gauri Shetye, Duc Nguyen, Mallique Qader, Angela C. Nugent, Enock Mpofu, Camarria Williams, Jonathon Rodriguez, Joanna E. Burdette, Sanghyun Cho, Scott G. Franzblau, Alessandra S. Eustáquio, Qibin Zhang, and Brian T. Murphy*

Cite This: *ACS Omega* 2024, 9, 44749−44759

Read Online

ACCESS | Metrics & More | Article Recommendations | Supporting Information

ABSTRACT: We established a university-community partnership with the Boys and Girls Clubs of Chicago (BGCC)—named *Chicago Antibiotic Discovery Lab*—to involve middle school students in antibiotic discovery research. In the course of working with a cohort of students from the BGCC, one student isolated a *Pseudomonas idahonensis* bacterium from a goose feces sample that produced a new cyclic lipodepsipeptide, which was characterized as orfamide N. Orfamide N is composed of ten mixed D/L-amino acids and a (*Z*)-3*R*-hydroxyhexadec-9-enoic acid residue. The planar structure of orfamide N was elucidated by one-dimensional (1D) and two-dimensional nuclear magnetic resonance (2D NMR), electrospray ionization-mass spectrometry (ESI-MS), and ozone-induced dissociation mass spectrometry (OzID-MS). The absolute configuration was determined by advanced Marfey's analysis, phylogenetic analysis of C-domains within the orfamide N biosynthetic gene cluster, and chiral high-performance liquid chromatography (HPLC) analysis of the hydrolyzed and reduced lipid tail. Orfamide N was cytotoxic against human melanoma and human ovarian cancer cells with IC_{50} values of 11.06 and 10.50 μM, respectively. Overall, we demonstrated it is possible to integrate educational outreach with high-end natural product discovery while strengthening the relationship between the university and the community it serves.

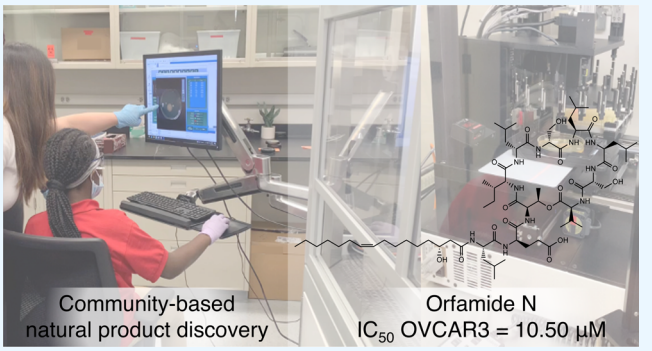

INTRODUCTION

Significant inequity exists in the educational resources available in low-income neighborhoods in Chicago, particularly those that serve student populations who are underrepresented in STEM. Although universities are a hub for STEM resources and mentorship connections, there is often a disconnect between higher-education institutions and the local communities they serve.[1] In an effort to engage students from underrepresented backgrounds in STEM, we established a university-community partnership with the Boys and Girls Clubs of Chicago (BGCC) to involve middle school students in antibiotic discovery research through a STEM outreach program, *Chicago Antibiotic Discovery Lab*. There are three central components to the 14-week program: field work, applied science experiments, and environmental literacy. Each week builds upon one another, all while a near-peer mentoring team links each module to different careers in the sciences. Middle school students build mentorship connections with graduate students or postdoctoral scientists, who help guide the project through joint decision-making throughout the program.

Students and their mentors employ our in-house semi-automated antibiotic discovery pipeline to explore their neighborhood for new bioactive compounds isolated from bacteria that they grew using high-throughput robotics. The pipeline employs a high-throughput colony-picking robot encased in a custom biosafety-level 2 cabinet, which allows students to safely perform several front-end processes such as bacterial growth, colony selection, and transfer of bacteria to multiwell bioassay plates. Importantly, the students perform research on samples they collect from their own neighborhood, which places their community in the center of high-end

Received: August 20, 2024
Revised: October 2, 2024
Accepted: October 11, 2024
Published: October 24, 2024

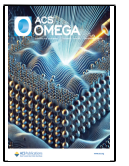

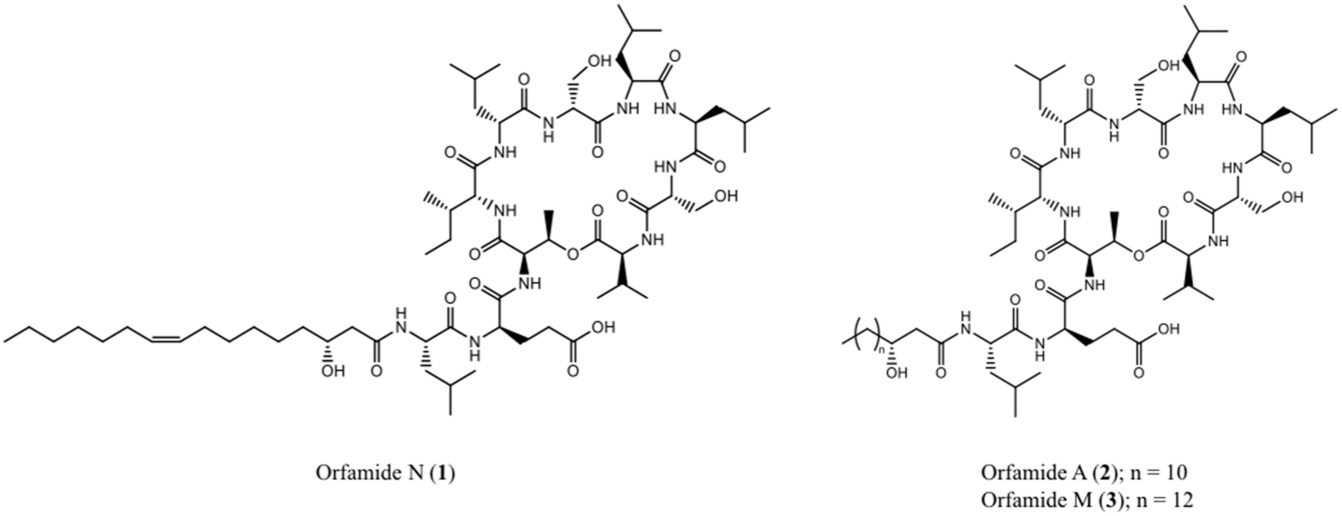

Figure 1. Structures isolated from *P. idahonensis* strain BGCFaB3.

biomedical sciences. This, in addition to having real intellectual input throughout each step of the process, instills a sense of ownership into their project. In the course of working with a cohort of students from the James R. Jordan BGCC, one student isolated a *Pseudomonas* sp. from a goose feces sample that produced a new cyclic lipodepsipeptide, which was characterized as orfamide N. Herein, we report the isolation, full structure characterization, and biological activity of orfamide N and show that it is possible to integrate educational outreach programs with high-end natural product discovery.

RESULTS AND DISCUSSION

Collection and Prioritization of Isolate BGCFaB3. Bacterial isolate BGCFaB3 was derived from a sample of goose feces collected by a middle school student researcher at Garfield Park Lagoon, Chicago. This isolate, in addition to 1195 others derived from 14 environmental samples, was screened using our high-throughput, in-house dual-sided agar plate assay.[2] Isolate BGCFaB3 exhibited growth inhibition activity of ≥90% against *Staphylococcus aureus* ATCC 29213. All hits were subjected to analysis on the IDBac bioinformatics platform to assess the degree of phylogenetic and natural product overlap; redundancies were removed and BGCFaB3 was selected for larger-scale fermentation.

Isolate BGCFaB3 was identified by whole genome phylogenetic analysis to be *Pseudomonas idahonensis* (Supporting Information (SI), Figure S17). After a 2 L fermentation in high nutrient media, the culture broth was extracted and subjected to successive reversed-phase chromatographic experiments. An antibiotic disk diffusion assay was used to guide the fractionation process (See SI, Figure S1 for a detailed fractionation tree). The only active fraction (BGCFaB3−6) was subjected to a second round of separation, resulting in 11 subfractions (SI, Figure S2). Upon analysis by ultraperformance liquid chromatography-tandem mass spectrometry (UPLC-MS/MS) and the dereplication platform Global Natural Product Social Molecular Networking (GNPS),[3−5] we identified the major subfractions 6−11 to contain MS fragmentation patterns similar to the orfamide family of cyclic lipopeptides (SI, Figure S3). Three of these subfractions (8, 9, and 11) yielded pure compounds that we putatively identified as orfamide A, orfamide M, and a new orfamide analog. Assuming these were the components responsible for antibiotic activity, our team proceeded with structure elucidation.

The structure of known orfamide A (**2**) was confirmed through analysis of high-resolution electrospray ionization mass spectrometry (HR-ESI-MS) in addition to a comparison of ^{1}H and ^{13}C NMR resonances to those published in literature (experimental 2D NMR spectra were acquired for reference as well).[6,7] These data were used to assist elucidation of the orfamide N structure (**1**), as differences between the two structures are present only in the lipid tail (Figure 1).

Structure Elucidation of Orfamide N. Compound **1** was suspected to be a new analog of the orfamide class based on a thorough literature search of the molecular weights of existing orfamide analogs and other structurally similar cyclic peptides. The molecular formula of **1** was determined by HR-ESI-MS to be $C_{66}H_{116}N_{10}O_{17}$, which has an unsaturation number of 14. The ^{1}H NMR spectrum in d_3-MeOH displayed resonances for exchangeable amide protons at δ_H 7.58−9.41 and overlapping α-proton signals at δ_H 3.87−4.47, while ^{13}C NMR spectra revealed the presence of 12 carbonyls at δ_C 170.94−177.06 (Table 1). All one bond ^{1}H−^{13}C correlations were established by a DEPT135-edited-HSQC NMR experiment, which determined the presence of 10 α-amino acid methines. These resonances are characteristic of the peptidic nature of **1**. The ^{1}H NMR spectrum also displayed overlapping resonances from δ_H 1.29−1.36 while the ^{13}C NMR spectra exhibited a cluster of aliphatic methylene signals from δ_C 28.17−32.95, suggesting the presence of a long-chain alkyl group in **1**. Additionally, 1D NMR and HSQC spectra revealed that **1** contained a double-bond with overlapping proton signals at δ_H 5.35 and two carbon signals δ_C 130.92 and 130.79.

The complete spin system of all amino acids in **1** was established by analysis of homonuclear correlation spectroscopy (COSY) and total correlation spectroscopy (TOCSY) spectra (Figure 2). These results, taken together with DEPT-edited-HSQC and HMBC NMR spectra, identified the following 10 amino acids in **1**: 4 Leu, 2 Ser, 1 Thr, 1 Ile, 1 Val, and 1 Glu (Figure 2). These 10 amino acids were equivalent to those present in **2**, which meant that the difference in planar structure composition between the two compounds was present only in the lipid tail. By subtracting all atoms accounted for by the 10 amino acid residues from the molecular formula of **1**, the remaining lipid tail portion of the

https://doi.org/10.1021/acsomega.4c07459
ACS Omega 2024, 9, 44749−44759

Table 1. ^{1}H (600 MHz) and ^{13}C (150 MHz) NMR Spectroscopic Data for Orfamide N (1) in d_3-MeOH

unit	position	δ_C, type	δ_H, mult. [J (Hz)]	unit	position	δ_C, type	δ_H, mult. [J (Hz)]
L-Leu1	1	175.80, C		L-Leu7	1	172.29, C	
	2	54.29, CH	4.00, m		2	53.69, CH	4.47, m
	3	40.69, CH_2	1.67, m		3	41.86, CH_2	1.80, m; 1.47, m
	4	25.87, CH	1.69, m		4	25.60, CH	1.74, m
	5	22.50, CH_3	0.95, m		5	21.59, CH_3	0.90, m
	6	23.23, CH_3[a]	0.98, m[a]		6	23.82, CH_3	0.96, m
	NH		8.66, brs		NH		7.94, m
D-Glu2	1	176.20, C		L-Leu8	1	174.95, C	
	2	177.06, C			2	54.34, CH	4.29, m
	3	56.55, CH	4.01, m		3	41.46, CH_2	1.72, m
	4	27.32, CH_2	2.10, m; 2.01, m		4	25.92, CH	1.67, m
	5	34.57, CH_2[b]	2.35, m		5	22.06, CH_3	0.91, m
	NH		9.41, brs		6	23.37, CH_3[a]	0.97, m[a]
					NH		7.90, m
D-*allo*-Thr3	1	173.11, C					
	2	60.85, CH	4.30, m	D-Ser9	1	172.29, C	
	3	70.66, CH	5.38, m		2	57.89, CH	4.28, m
	4	18.68, CH_3	1.39, d (5.9)		3	62.62, CH_2	3.89, m; 3.81, dd (11.3; 4.2)
	NH		8.20, d (7.2)		NH		8.04, brs
D-*allo*-Ile4	1	175.19, C		L-Val10	1	170.94, C	
	2	62.62, CH	3.87, m		2	59.69, CH	4.33, m
	3	37.06, CH	2.05, m		3	31.46, CH	2.16, m
	4	27.01, CH_2	1.46, m; 1.18, m		4	19.83, CH_3	0.87, m
	5	11.77, CH_3	0.91, m		5	18.95, CH_3	0.82, d (6.7)
	6	16.40, CH_3	0.98, m		NH		7.68, m
	NH		7.58, brs				
				3′*R*−OH-hexadec-9-enoic acid	1′	175.02, C	
D-Leu5	1	175.50, C			2′	44.52, CH_2	2.43, m; 2.40, m
	2	54.97, CH	4.17, m		3′	69.89, CH	4.08, m
	3	40.89, CH_2	1.79, m; 1.56, m		4′	38.55, CH_2	1.50, m
	4	25.83, CH	1.79, m		5′	26.62, CH_2	1.50, m
	5	21.14, CH_3	0.87, m		6′	30.46, CH_2[a]	1.28, m[a]
	6	23.69, CH_3[a]	0.93, m[a]		7′	30.06, CH_2[a]	1.36, m[a]
	NH		7.80, brs		8′	28.17, CH_2	2.04, m
					9′	130.92, CH	5.35, m
D-Ser6	1	172.98, C			10′	130.79, CH	5.35, m
	2	58.33, CH	4.37, m		11′	28.17, CH_2	2.04, m
	3	62.85, CH_2	3.95, dd (11.6; 5.7);		12′	30.91, CH_2[a]	1.28, m[a]
			3.89, m		13′	30.85, CH_2[a]	1.28, m[a]
	NH		7.71, brs		14′	32.95, CH_2[aa]	1.28, m[a]
					15′	23.73, CH_2	1.31, m
					16′	14.46, CH_3	0.89, m

[a]These four sets of chemical shifts are interchangeable. [b]Shift acquired via analysis of HSQC data.

molecule was determined to contain $C_{16}H_{29}O_2$. Using ^{13}C and DEPT135-edited-HSQC NMR data, these remaining carbons were confirmed to consist of one carbonyl (δ_C 175.02), one carbinol methine (δ_C 69.89), one methyl (δ_C 14.46), two vinylic carbons (δ_C 130.92 and 130.79), and 11 aliphatic methylene carbons (δ_C 23.73−44.52). Key COSY correlations from H-3′ (δ_H 4.08) to $H_{2\alpha}$-2′ (δ_H 2.40) and H_2-4′ (δ_H 1.50), and HMBC correlations between $H_{2\alpha}$-2′ and C-1′ (δ_C 175.02), identified the fatty acid fragment as 3′−OH-hexadecenoic acid (C16:1). Thus, the C16:1 fatty acid fragment of **1** accurately accounted for the difference of 26 mass units and one double-bond equivalence between the two molecules.

The composition and sequence of amino acids in **1** were confirmed by MS/MS analysis of the intact peptide as well as the linearized methyl ester of **1** (Figure 3). Analysis of the y- and b-series fragment ions suggested the following sequence: C16:1-Leu1-Glu2-Thr3-Ile4-Leu5-Ser6-Leu7-Leu8-Ser9-Val10. A few key HMBC correlations also supported this sequence of amino acid residues (Figure 2). Furthermore, this is consistent with the product peptide predicted based on the specificity of the adenylation domains (A) in antiSMASH (Figure 4).

To determine the absolute configuration of each amino acid, the acid hydrolysate of **1** was subjected to advanced Marfey's analysis to yield 2 D-Ser, 1 D-*allo*-Thr, 1 L-Val, 1 D-Glu, 1 D-*allo*-Ile or D-Ile, 3 L-Leu, and 1 D-Leu (SI, Figure S20).[8] To resolve the configuration of the remaining Ile residue, the underivatized hydrolysate of **1** was subjected to chiral HPLC analysis. A comparison of the retention time to Ile standards showed it to be of D-*allo* configuration (SI, Figure S19). The stereoconfiguration of amino acids was also supported by AntiSMASH prediction of the condensation (C) domains at

https://doi.org/10.1021/acsomega.4c07459
ACS Omega 2024, 9, 44749−44759

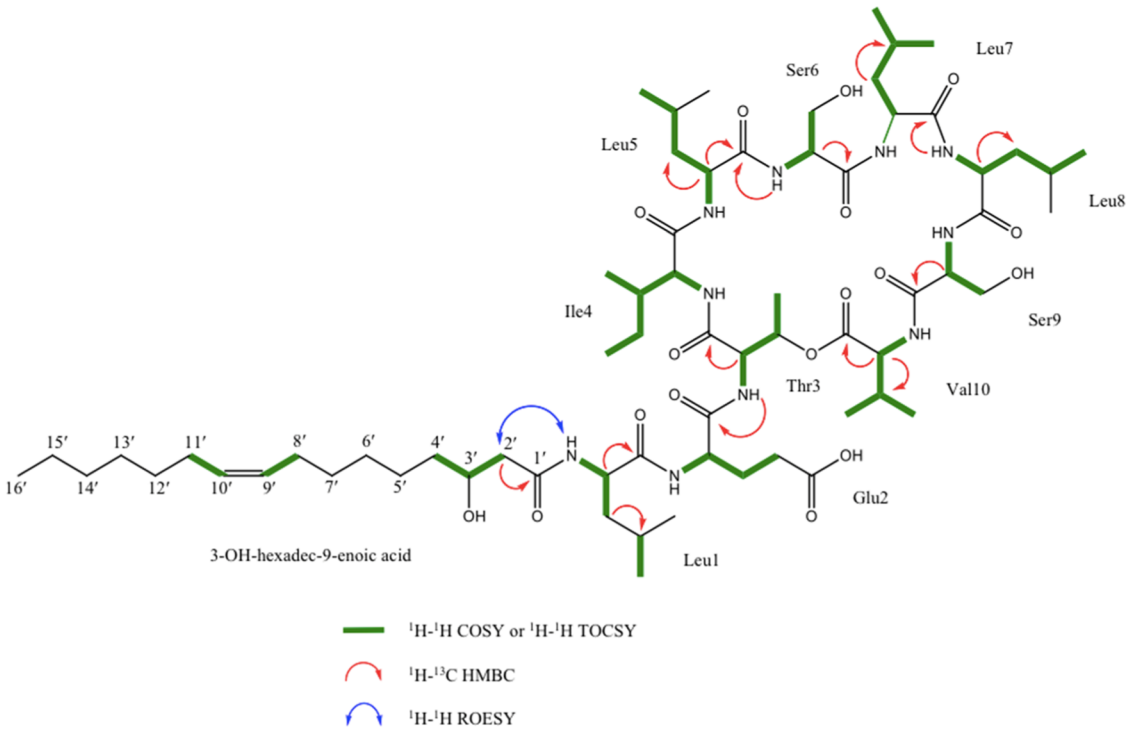

Figure 2. Key 2D NMR correlations for orfamide N (**1**).

each module (Figure 4). However, the C-domains at module 2 (C-2) and module 6 (C-6) were classified as C_{DUAL}. In order to resolve the position of the single D-Leu in **1**, a C-domain phylogenetic tree and sequence alignment was performed (SI, Figure S18). C-2 presented two mutations in the catalytic region essential for C_{DUAL} activity, suggesting the domain is incapable of performing the epimerization of L-Leu at module 1. On the other hand, this region was fully conserved for C-6, suggesting the epimerization of L-Leu to D-Leu at module 5. Our phylogenetic prediction is also supported by a comparison to published ^{1}H NMR data generated by Bando et al. where L- and D-leucines were substituted by total synthesis.[7] The amino acid stereoassignments in orfamide N are consistent with the 12 other published orfamides (B-M) that report a D-leucine at position 5.[19] Thus, the configuration of the amino acids in **1** was assigned as C16:1-L-Leu1-D-Glu2-D-*allo*-Thr3-D-*allo*-Ile4-D-Leu5-D-Ser6-L-Leu7-L-Leu8-D-Ser9-L-Val10.

Ozone-induced dissociation mass spectrometry (OzID-MS) was used to annotate the position of the double bond in the lipid tail.[9−11] The mechanism of OzID-MS is based on the selective reaction between C═C and ozone gas, which results in the formation of characteristic aldehyde product ions. The difference in the corresponding m/z of the precursor and product ions (neutral losses) is diagnostic of carbon−carbon double bond positions.[12,13] When performing the OzID-MS on compound **1**, a product ion (m/z 1223.7438 $[M + H]^+$, t_R= 14.48 min) was identified at the same retention time of **1** (m/z 1321.8591 $[M + H]^+$, 1338.8852 $[M+NH_4]^+$). This product was absent when the LC-MS analysis of **1** was carried out under the same experimental conditions but without the exposure to ozone (Figure 5). In addition, the detected isotopic envelopes of **1** and its aldehyde product matched their calculated isotopic abundances (Figure 5). Based on the neutral loss of 82 Da upon the exposure to ozone, compound **1** was concluded to have a double bond located between C-9′ and C-10′ in the lipid tail. This notion was further confirmed by the analysis of the MS^2 spectra of **1** and its ozone-induced aldehyde product ion, which showed the presence of key MS/MS fragments of **1** and the respective mass shift introduced by the aldehyde product (Figure 6).[14]

As is often observed in midchain double bond ^{1}H NMR signals in lipids, the minimal chemical shift difference between alkenyl protons produces a complex signal that is not well resolved or susceptible to first-order analysis, making it difficult to measure the corresponding coupling constant.[15] However, we determined that the largest ^{1}H/^{1}H coupling constant possible was 11 Hz. This is similar to the coupling constants (J_{AB}) described for n-9 *cis* double bonds in fatty acid methyl esters determined by selective homonuclear decoupling experiments, which ranged from 10.8−11.0 Hz, while J_{AB} for their n-9 *trans* double bond counterparts ranged from 15.3−15.4 Hz.[16] Furthermore, analysis of ^{13}C NMR shifts is commonly used for identifying configurations of such double bonds. The allylic carbons in orfamide N (δ_C 28.2) closely resemble the published mean for *cis* double bonds (δ_C 27.3) than that for *trans* double bonds (δ_C 32.6).[17] Thus, we were able to unequivocally assign the double bond to be in the *cis* configuration.

The configuration of C-3′ in the 3′-hydroxy-hexadecanoic acid moiety was determined using the following steps: (1) acid hydrolysis of **1** and extraction with chloroform to obtain the free 3-hydroxy-hexadec-9-enoic acid, (2) catalytic hydrogenation to saturate the double bond in the lipid tail to obtain 3-hydroxy-hexadecanoic acid, and (3) comparison of retention times to a 3*R*/*S*-hydroxy-hexadecanoic acid standard by chiral liquid chromatography−mass spectrometry (LC−MS) analysis using a previously established method.[18] The retention time of the major peak from the extracted ion chromatogram for experimental 3-hydroxy-hexadecanoic acid (t_R= 18.3 min) matched that of the 3*R*-hydroxy-hexadecanoic acid standard

https://doi.org/10.1021/acsomega.4c07459
ACS Omega 2024, 9, 44749−44759

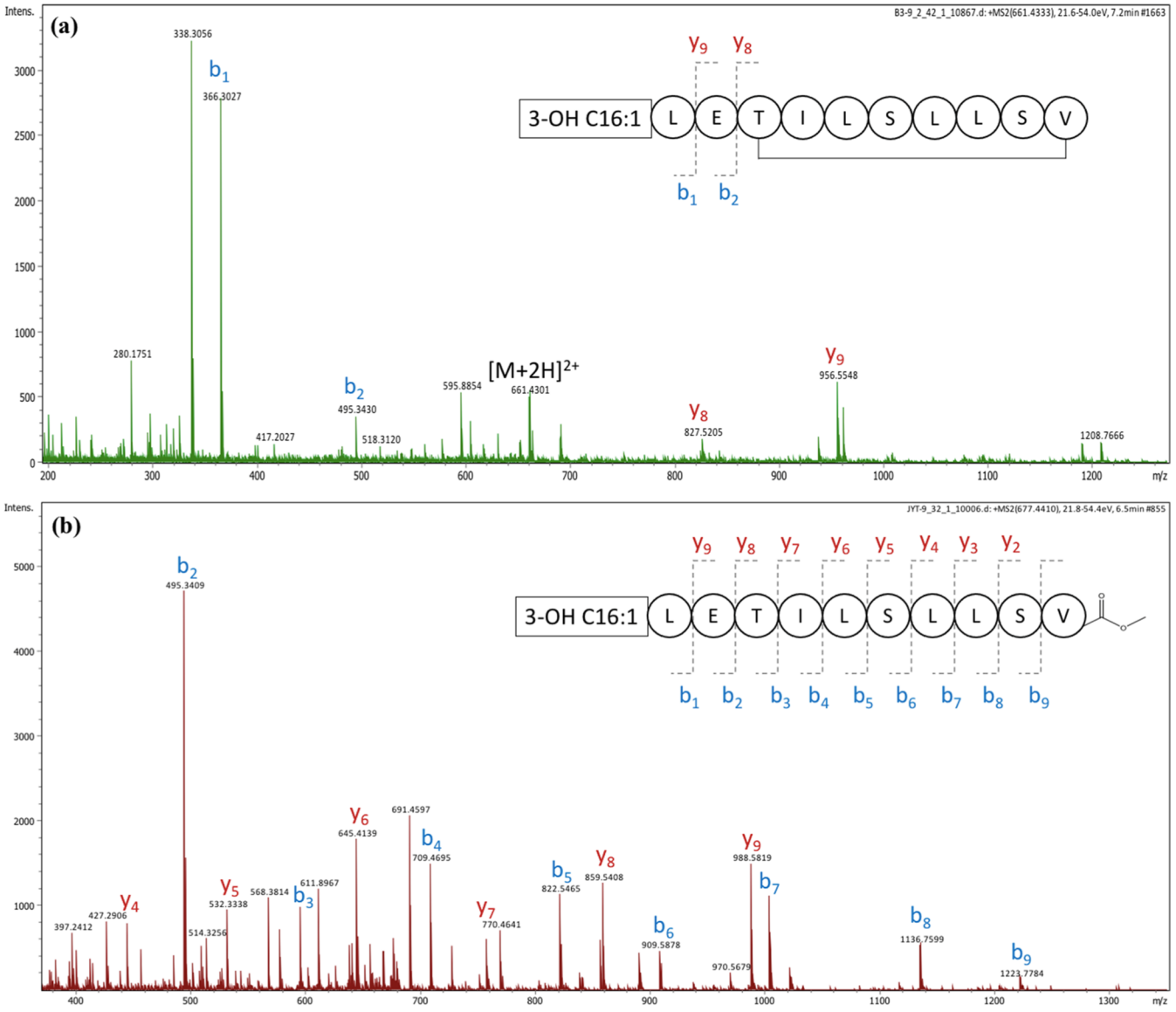

Figure 3. MS/MS fragmentation pattern for (a) orfamide N and (b) orfamide N methyl ester.

(t_R= 18.4 min) (see SI, Figure S21). Thus, the configuration of the hydroxyl group in the lipid side chain was determined to be *R*. This is consistent with the configuration of *β*-hydroxy acids reported in other analogs of the orfamide-family of cyclic lipopeptides.

Biological Activity of Orfamide N. Several cyclic lipodepsipeptides from *Pseudomonas* spp. have been reported to possess antibacterial activity and antiproliferation effects on human cancer cell-lines.[20] Additionally, various orfamides have shown cytotoxic activity in eukaryotic cells including insecticidal, antifungal, and algicidal activity.[6,7,28,29] As such, we decided to investigate the antibacterial and anticancer potential of **1**. We did not observe significant antibacterial activity for compounds **1** and **2** when screened against a diverse panel of pathogenic bacteria (SI, Figure S22), though compound **1** displayed IC_{50} values of 11.06 and 10.50 μM against human melanoma MDA-MB-435 and human ovarian cancer cells OVCAR3, respectively. Compound **2** exhibited a similar activity profile to that of **1** (Table 2).

Conclusions. Extensive fractionation of *P. idahonensis* BGCFaB3 led to the discovery of a new cytotoxic lipodepsipeptide. Efforts are underway to determine the compound(s) responsible for the original antibiotic activity observed against *S. aureus* ATCC 29213, though in this effort we report the isolation, structure elucidation, and bioactivity of a new natural product orfamide N. This new cyclic lipodepsipeptide was discovered through a community-based natural product discovery outreach program with middle school students from populations that are underrepresented in STEM. We demonstrated that educational outreach initiatives can be integrated into high-end biomedical research projects via university-community partnerships.

EXPERIMENTAL SECTION

General Experimental Procedures. NMR spectra were obtained on a Bruker 600 (150) MHz AVANCE III NMR spectrometer equipped with a 5 mm TCI cryogenic inverse probe with *z*-axis pfg and TopSpin version 3.2 operating software, at the University of Illinois at Chicago Center for Structural Biology. Chemical shifts (δ) are given in ppm and coupling constants (J) are reported in Hz. ^{1}H and ^{13}C NMR chemical shifts were referenced to d_3-MeOH (δ_H 3.31 ppm and

https://doi.org/10.1021/acsomega.4c07459
ACS Omega 2024, 9, 44749−44759

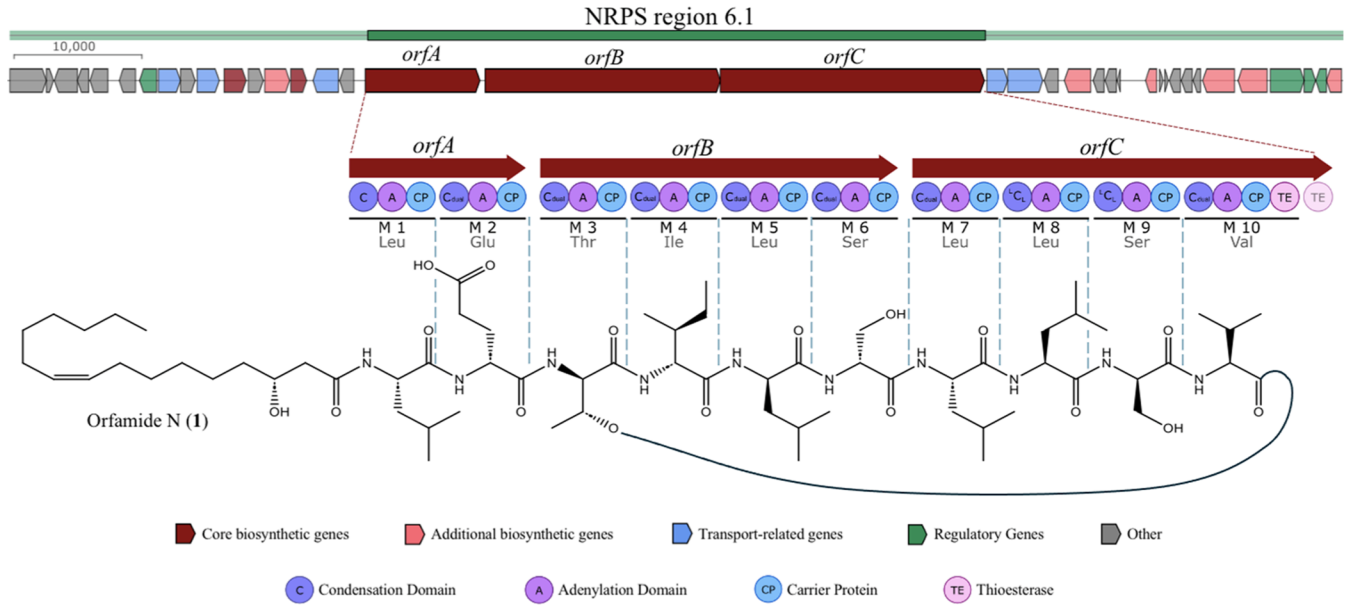

Figure 4. Predicted biosynthesis of orfamide N, highlighting region 6.1, which comprises three NRPS (*orfA*, *orf B*, and *orf C*) and several putative accessory genes. The amino acid incorporated at each of the ten modules in the NRPS genes was predicted based on the specificity of the adenylation domains (A). A thioesterase (TE) domain at the end of module 10 cyclizes the product and releases the depsipeptide. The configuration of the amino acids was predicted based on the type of condensation domains (C) (SI, Figure S18).

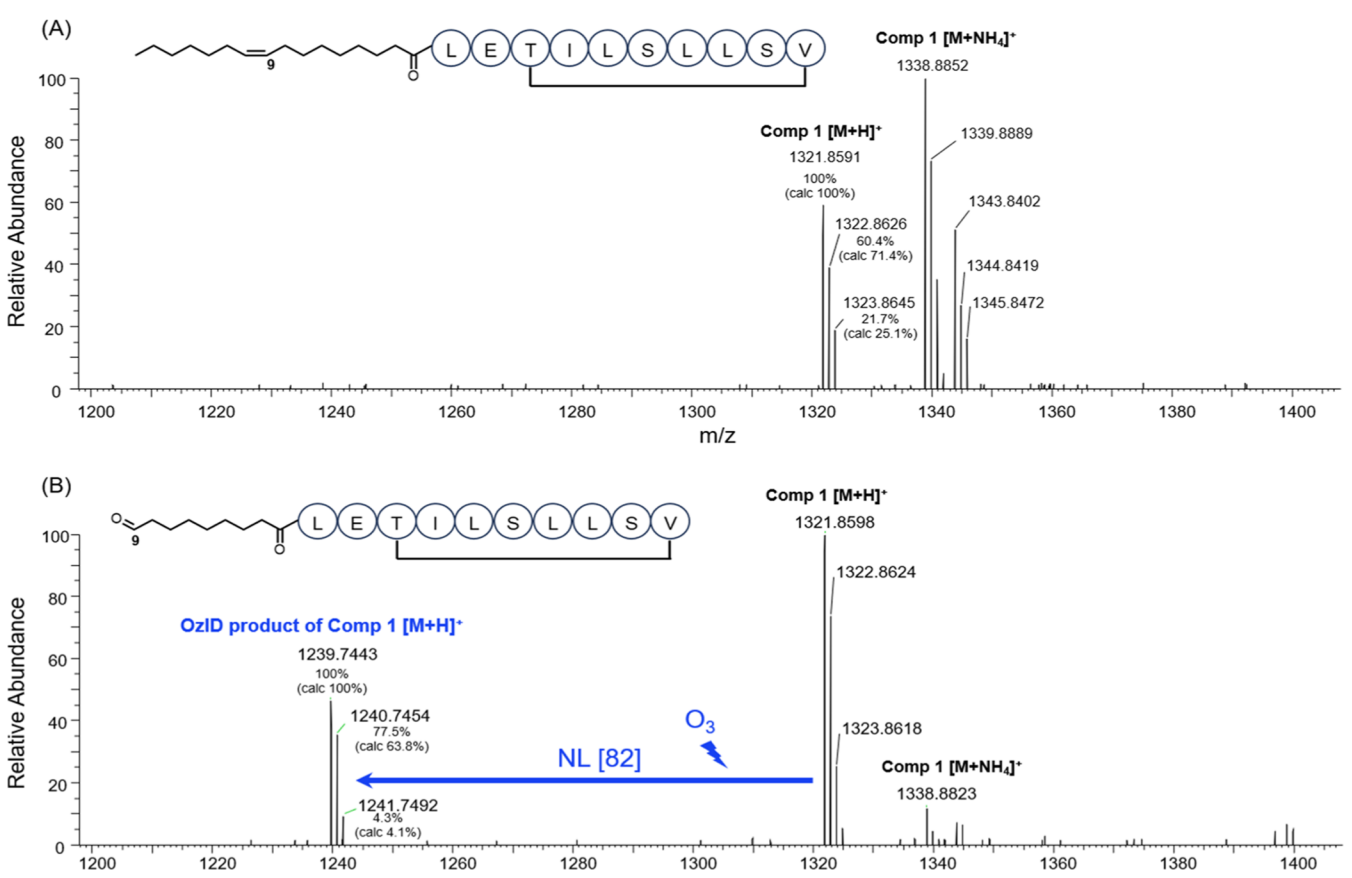

Figure 5. OzID-MS spectra of orfamide N (A) without and (B) with the exposure to ozone.

δ_C 49.0 ppm, respectively). High-resolution mass spectra, LC-MS data, and MS/MS fragmentation spectra were obtained on a Bruker COMPACT ESIQTOF mass spectrometer at the University of Illinois at Chicago. Flash chromatography was performed using a Teledyne Isco Combiflash system with ELSD and ultraviolet (UV) detection. Analytical HPLC data were obtained using a Hewlett-Packard Agilent 1100 system controller and pumps with a Model G1315A diode array detector (DAD) and Shimadzu ELSD LTII light scattering detector. MALDI-TOF MS analyses were carried out a rapifleX

https://doi.org/10.1021/acsomega.4c07459
ACS Omega 2024, 9, 44749−44759

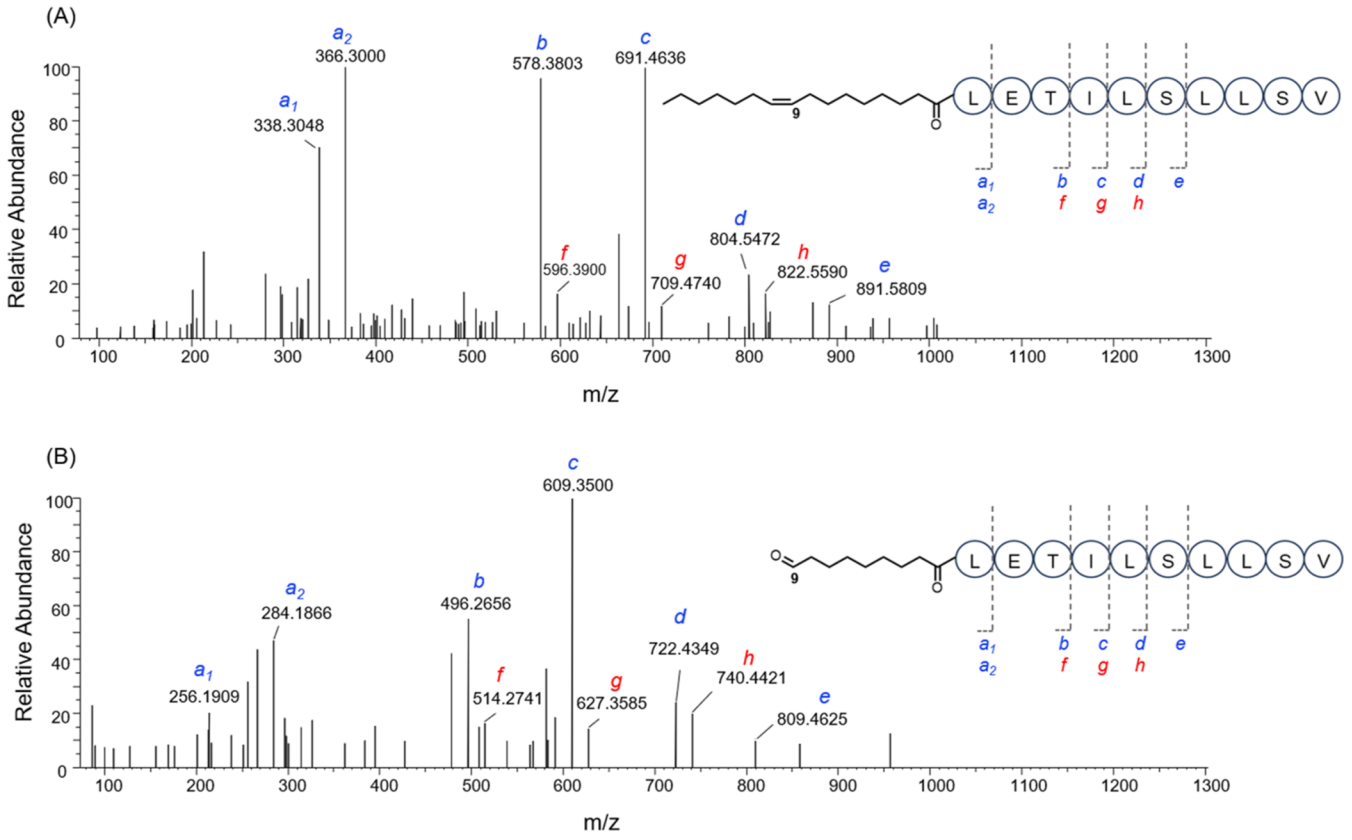

Figure 6. MS/MS spectra for (A) orfamide N and (B) its ozone-induced aldehyde product. The MS^2 fragments f-h were generated after the cleavage of **1** at the ester bond, while the MS^2 fragments b-e were vinylic derivatives after water elimination from threonine following the cleavage of the ester bond in **1**.

Table 2. Results of Cytotoxicity Assay[a]

	results (% cell viability)	
	OVCAR3 (μM)	MDA-MB-435 (μM)
orfamide N (**1**)	10.50 ± 4.17	11.06 ± 5.00
orfamide A (**2**)	11.44 ± 3.76	11.62 ± 3.92
taxol (nM)	2.129 ± 0.488	5.580 ± 1.298

[a]Cells were plated and treated with taxol, compound **1**, or compound **2** for 72 h. Dose-response curves were generated for OVCAR3 and MDA-MD-435. IC_{50} values were generated from dose-response curves. Each experiment was performed in three biological replicates and data represent triplicate values ± SEM.

MALDI Tissuetyper mass spectrometer (Bruker Daltonics) equipped with a smartbeam 3D laser (355 nm). Automated data acquisitions were performed using flexControl software v. 4.0.46.0 (Bruker Daltonics) and flexAnalysis software v. 3.4. MALD-TOF spectra were corrected with external Bruker Daltonics bacterial test standard and peptide calibration standard. Semipreparative HPLC was performed using a Shimadzu LC20AB system equipped with a SPD 20A UV/vis detector. Samples were dried using a Genevac EZ-2 series personal evaporator. All solvents were spectroscopic grade. NMR spectra were acquired in d_3-MeOH (99.8 atom % D, Sigma-Aldrich).

Summary of Chicago Antibiotic Discovery Lab Workflow. All experiments are performed under the guidance of graduate student or postdoctoral scientist volunteer mentors. Each student collected 3 samples of their choice from Garfield Park in Chicago, IL. Students pretreated and diluted their samples before plating each one on three different media types (A1, R2A, and TSA). While their bacteria incubated, they practiced block programming on LEGO EV3 modules in preparation for robot operation. When their environmental diversity plates exhibited sufficient bacterial growth, students programmed and operated the Hudson Robotics RapidPickMP to pick all distinguishable colonies from their environmental diversity plates and transfer them onto dual-sided agar plate assay (DAPA) bioassay plates. DAPA screening was performed following previously published methods.[2] Every colony was screened against *Pseudomonas aeruginosa* (ATCC 10145 GFP) and *S. aureus* (ATCC 29213). These pathogens were chosen to represent one gram-negative and one gram-positive strain that grow well under our lab conditions. Students then interpreted bioassay data and compiled hits, defined here as exhibiting growth inhibition activity of ≥90%. Hits were transferred to A1 agar media and incubated for 7 days in preparation for MALDI-TOF MS data acquisition. MALDI-TOF MS data was acquired for all hit isolates and uploaded to the MS-based bioinformatics tool IDBac following previously established protocols.[21] IDBac metabolite association networks (MANs) were created by retaining peaks with a signal-to-noise ratio above 4 and that occurred in greater than 70% of replicate spectra. Peaks that occurred below 200 m/z or above 2000 m/z were removed from the analysis. Students analyzed IDBac-generated MANs and protein dendrograms in order to prioritize their hits based on potential natural product and phylogenetic redundancy, respectively, and generated a list of final leads.[22]

https://doi.org/10.1021/acsomega.4c07459
ACS Omega 2024, 9, 44749−44759

Synthesis of Orfamide N Methyl Ester by Methanolysis. Twenty μL of NaOMe (0.5 M in MeOH) was added to 0.1 mg of orfamide N dissolved in 0.5 mL of MeOH in a sealed vial and left at room temperature for 1 h. MS/MS fragmentation spectra of the product was recorded on a Bruker COMPACT ESIQTOF with an Agilent Poroshell 120 EC-C18 column (2.1 × 50 mm^2, 1.9 μm) at 0.5 mL/min using a gradient of 10−90% B over 9 min (A = water with 0.01% formic acid; B = acetonitrile with 0.01% formic acid). HRESI-TOF MS orfamide N m/z 661.4333 $[M + 2H]^{2+}$ ($M = C_{66}H_{116}N_{10}O_{17}$; calcd. for $[M + H]^+$: 1321.8593; calcd. for $[M + 2H]^{2+}$: 661.4333; Figure 3); orfamide N methyl ester m/z 661.4313 $[M + 2H]^{2+}$ ($M = C_{67}H_{120}N_{10}O_{18}$; calcd. for $[M + H]^+$: 1353.8855; calcd. for $[M + 2H]^{2+}$: 677.4464; Figure 3).

Acid Hydrolysis and FDAA Derivatization for Advanced Marfey's Analysis. 50 μg of orfamide N (**1**) was hydrolyzed with 100 μL of 6 M HCl at 100 °C in a sealed vial for 18 h to release amino acid residues, after which the hydrolysate was concentrated to dryness. The hydrolysate was treated with 20 μL of 1 M $NaHCO_3$ (Fisher Chemicals) and 100 μL of 1-fluoro-2−4-dinitrophenyl-5-L-alanine amide (L-FDAA, 10 mg/mL in acetone, Thermo Fisher) at 40 °C for 1 h. The reaction was then neutralized with 20 μL of 1 M HCl and filtered (0.45 μm PTFE). An aliquot (2 μL) of the resulting solution was analyzed by UPLC-DAD-ESIMS with an Agilent Poroshell 120 EC-C18 column (2.1 × 50 mm^2, 1.9 μm) at 0.5 mL/min using a gradient of 25−50% B over 10 min (A = water with 0.01% formic acid; B = acetonitrile with 0.01% formic acid). 50 μL of each amino acid standard (50 mM in H_2O, Fisher Chemicals) was derivatized and analyzed in the same fashion as **1**. Retention times were measured by UPLC-DAD-ESIMS extracted ion chromatograms. The retention times of derivatized amino acids in **1** were then compared with those of derivatized amino acid standards (SI, Figure S20).

Chiral HPLC Analysis of Isoleucine Residues. Chiral HPLC analysis of the underivatized hydrolysate of **1** was performed using a Phenomenex Chirex 3126 D-penicillamine column (4.6 × 250 mm^2) with an isocratic flow of 1 mM copper(II) sulfate in water/isopropanol (95:5) at 1 mL/min. The retention time of the Ile residue in orfamide N (**1**) was compared to that of D- and D-*allo*-Ile standards (SI, Figure S19A). Retention times were measured by HPLC at 254 nm. Identifications were confirmed by coinjection with standards. (SI, Figure S19B).

Catalytic Hydrogenation of 3-OH-Hexadec-9-enoic Acid. 50 μg of orfamide N was hydrolyzed with 100 μL of 6 M HCl at 100 °C in a sealed vial for 20 h. The free 3-OH-hexadec-9-enoic acid was obtained from the hydrolysate by liquid−liquid extraction with chloroform. The chloroform layer was concentrated to dryness, and the residue was dissolved in 2 mL of methanol. Saturation of the double bond in 3-OH-hexadec-9-enoic acid was performed by catalytic hydrogenation with 5 mg of palladium on carbon (Pd/C) and a constant flow of hydrogen gas over 18 h at 25 °C. The reaction product was filtered through Celite and concentrated to dryness to obtain 3-hydroxy-hexadecanoic acid.

Chiral UPLC−ESI-MS Analysis of the Fatty Acid Portion of 1. The product from the hydrogenation reaction, 3-hydroxy-hexadecanoic acid, was used to determine the absolute configuration of the 3′-hydroxyl moiety in **1**. Chiral LC-MS analysis of the hydrogenation product was performed with a Chiralpak-IA-U column (3 × 100 mm^2, 1.6 μm) at 0.3 mL/min using a gradient of 10−100% B over 20 min (A = water with 0.01% formic acid; B = acetonitrile with 0.01% formic acid). The ESI source was operated in negative ionization mode at 220 °C and 3 bar with a dry gas flow of 12 L/min. Retention times were compared to a 3-*RS*-hydroxyhexadecanoic acid standard (Cayman Chemical) (SI, Figure S21). It was previously reported that the *R*-enantiomer elutes after the *S*-enantiomer using the same column and gradient solvent system.[18]

OzID-MS Analysis of 1. The OzID-MS experiment was performed on a Q Exactive HF mass spectrometer (ThermoFisher Scientific) as reported previously with some modifications,[9−11] coupled to a Vanquish Horizon UHPLC (ThermoFisher Scientific) for front-end separation. A stock solution of orfamide N (1, 4 μg/mL) was prepared in MeOH and 5 μL was subjected to the LC-MS analysis with and without the exposure to ozone. An ACQUITY Premier CSH C18 column (100 × 2.1 mm^2, 1.7 μm) was used at a flow rate of 200 μL/min and the following gradient: 0.0 min (5% B), 5.0−25.0 min (95% B). Prior to each injection, the LC column was equilibrated for 5 min at 5% solvent B. Solvents A and B consisted of water and ACN, respectively, and both were supplemented with 0.1% formic acid. The following parameters were set for the mass spectrometer: 20 and 1 Arb, 250 and 300 °C, and 50% for sheath gas, sweep gas, ion transfer tube, vaporizer temperature, and S-lens RF level, respectively. The aux gas was set at 5 Arb in positive mode. The ion source was operated using heated ESI with an ion spray voltage set at 3500 V in. Mass spectra were acquired in the scan range of 200−1500 m/z at a mass resolution of 120k (at 200 m/z), followed by data-dependent MS/MS with a mass resolution of 30k (at 200 m/z) for the 10 most abundant ions. The AGC targets were 1e6 and 1e5 in full-scan MS and dd-MS^2, respectively. The maximum injection time was set at 75 ms for both the full-scan MS and dd-MS^2. A dynamic exclusion of 8s and an isolation window of 1.0 m/z were used when acquiring the dd-MS^2 data. Moreover, a stepped collision energy of 25 and 30 was applied when collecting the dd-MS^2 data. An Absolute Ozone generator (Edmonton, Canada) was used to supply ozone and operated following manufacturer's instructions.

Cytotoxicity Assay. Human melanoma cells MDA-MB-435 and human ovarian cancer cells OVCAR3 were purchased from the American Type Culture Collection (Manassas, VA). Both cell lines were propagated at 37 °C in 5% CO_2, with MDA-MB-435 and OVCAR3 in RPMI 1640 medium, both supplemented with fetal bovine serum (10%), penicillin (100 units/mL), and streptomycin (100 μg/mL). Cells in log phase growth were harvested by trypsinization followed by two washing steps to remove all traces of enzyme. A total of 5000 cells were seeded per well of a 96-well clear, flat-bottom plate (Microtest 96, Falcon) and incubated overnight (37 °C in 5% CO_2). Samples dissolved in DMSO were then diluted and added to the appropriate wells. The cells were incubated in the presence of test substance for 72 h at 37 °C and evaluated for viability with a commercial absorbance assay (CellTiter 96 AQ_{ueous} One Solution Cell Proliferation Assay, Promega Corp, Madison, WI) that measured viable cells.

Strain Identification by Whole Genome Sequencing. The genomic DNA of the isolate BGCFaB3 was extracted from 2 mL of overnight culture using the GeneElute Bacterial Genomic DNA Kit (Sigma). The whole genome was sequenced by Illumina (seqcenter, Pittsburgh, PA), and the short reading assembly was performed with unicycler.[23] Strain identification was performed using the Type (Strain) Genome

https://doi.org/10.1021/acsomega.4c07459
ACS Omega 2024, 9, 44749−44759

Server (TYGS),[24] which extracts and BLASTs the 16S rRNA of the provided sequence, identifying the 10 closest strains on the NCBI database. The whole genome sequence of the selected strains is compared by calculating the Genome Blast Distance Phylogeny (GBDP) to define the closest relatives of the BGCFaB3 strain. The isolate (BGCFaB3) was identified to be *P. idahonensis* (SI, Figure S17).

Biosynthetic Gene Cluster Identification. The genome was analyzed in AntiSMASH 7.1 to identify all the possible biosynthetic gene clusters (BGC) present in the 29 contigs.[25] AntiSMASH analysis showed the presence of 21 regions with putative BGCs. Region 6.1 was annotated as a non-ribosomal synthetase that shared 88% gene similarity with a known BGC from *Pseudomonas protegens* Pf-5, responsible for the biosynthesis of the cyclic depsipeptides orfamide A and C. Nucleotide and amino acid alignment and the phylogenetic tree of condensation domains were analyzed in Geneious Prime 2023.2.1.

Isolation of Orfamide N. Isolate BGCFaB3 was grown in 2 L of A1 media at 25 °C while shaking at 220 rpm. On day 5, the extracellular secondary metabolites were absorbed from the fermentation broth using 1:1 Amberlite XAD-16 and 7HP polymeric resins, followed by extraction with 1:1 acetone:methanol. The solvent was dried under air to afford 0.85 g of extract. It was then cleaned up using C18 solid phase extraction to afford 0.75 g of extract, which was then suspended in MeOH and added dropwise onto 1.0 g of Celite. The organic solvent was evaporated under air before loading the dried Celite into a cartridge on a RediSep Gold C18 (50 g) column and separated by flash chromatography at 40 mL/min using a gradient of 10−100% B over 25 min (A = water +0.1% formic acid; B = methanol +0.1% formic acid). Upon a Kirby-Bauer disk diffusion assay against *S. aureus* ATCC 29123, only fraction 6 was active (100 μg/disk).[26] After method development on an analytical Luna C18 HPLC (250 × 4.6, 5 μm) column, fraction 6 was separated by semipreparative HPLC with a Luna C18 (250 × 10 mm, 5 μm) column at 3.5 mL/min using a gradient of 85−100% B over 45 min (A = water +0.1% formic acid; B = acetonitrile +0.1% formic acid) to yield compound **1** (t_R 31.3 min, 13.77 mg, Figure S2), compound **2** (t_R 33.5 min, 5.27 mg, Figure S2), and compound **3** (t_R 46.5 min, 6.38 mg, Figure S2). See SI, Figure S1 for a detailed fractionation tree.

Orfamide N (1). Orfamide N was isolated as an amorphous solid (5.27 mg). $[\alpha]_D^{20}$ = +2.5° (*c* 0.4 MeOH); UV (MeOH) λmax (log ε) 210 nm (1.3); ^{1}H NMR (600 MHz, d_3-MeOH) and ^{13}C NMR (150 MHz, d_3-MeOH), see Table 2, Figures S10 and S11. For complete two-dimensional NMR data, see Figures S12−S16. All raw NMR data files were deposited in the open access Natural Products Magnetic Resonance Database (NP-MRD ID NP0333636).[27] HRESI-TOF MS *m*/*z* 661.4313 $[M + 2H]^{2+}$ ($M = C_{66}H_{116}N_{10}O_{17}$; calcd. for $[M + H]^+$: 1321.8593; calcd. for $[M + 2H]^{2+}$: 661.4333; Figure S9).

Orfamide A (2). Orfamide A was isolated as an amorphous solid (13.77 mg). ^{1}H NMR (600 MHz, d_3-MeOH) and ^{13}C NMR (150 MHz, d_3-MeOH), see Figure S5. Two-dimensional NMR data see Figure S6. HRESI-TOF MS *m*/*z* 648.4241 $[M + 2H]^{2+}$ ($M = C_{64}H_{114}N_{10}O_{17}$; calcd. for $[M + H]^+$: 1295.8436; calcd. for $[M + 2H]^{2+}$: 648.4254; Figure S4).

Orfamide M (3). Orfamide M was isolated as an amorphous solid (6.38 mg). ^{1}H NMR (600 MHz, d_3-MeOH) and ^{13}C NMR (150 MHz, d_3-MeOH), see Figure S8. HRESI-TOF MS *m*/*z* 662.4412 $[M + 2H]^{2+}$ ($M = C_{66}H_{118}N_{10}O_{17}$; calcd. for $[M + H]^+$: 1323.8749; calcd. for $[M + 2H]^{2+}$: 662.4411; Figure S7).

■ ASSOCIATED CONTENT

Supporting Information

The Supporting Information is available free of charge at https://pubs.acs.org/doi/10.1021/acsomega.4c07459.

Spectroscopic data, consisting of one-dimensional NMR data and HR-qTOF-MS/MS spectra of **1**, **2**, and **3**, two-dimensional NMR data of **1** and **2;** bioassay data; and other materials (PDF)

Accession Codes

The assembled genome sequence of*P. idahonensis*BGCFaB3 has been deposited to GenBank under the accession number JBHGHH000000000. Raw sequence reads were submitted to SRA under the Biosample number SAMN43586470 and Bioproject number PRJNA1159859.

■ AUTHOR INFORMATION

Corresponding Author

Brian T. Murphy − *Department of Pharmaceutical Sciences, Center for Biomolecular Sciences, College of Pharmacy, University of Illinois at Chicago, Chicago, Illinois 60612, United States;* orcid.org/0000-0002-1372-3887; Phone: (312) 413-9057; Email: btmurphy@uic.edu

Authors

Jin Yi Tan − *Department of Pharmaceutical Sciences, Center for Biomolecular Sciences, College of Pharmacy, University of Illinois at Chicago, Chicago, Illinois 60612, United States*

Mario Augustinović − *Department of Pharmaceutical Sciences, Center for Biomolecular Sciences, College of Pharmacy, University of Illinois at Chicago, Chicago, Illinois 60612, United States*

Ashraf M. Omar − *Center for Translational Biomedical Research, University of North Carolina at Greensboro, Greensboro, North Carolina 27412, United States*

Vitor B. Lourenzon − *Department of Pharmaceutical Sciences, Center for Biomolecular Sciences, College of Pharmacy, University of Illinois at Chicago, Chicago, Illinois 60612, United States*

Nyssa Krull − *Department of Pharmaceutical Sciences, Center for Biomolecular Sciences, College of Pharmacy, University of Illinois at Chicago, Chicago, Illinois 60612, United States*

Xochitl Lopez − *Department of Pharmaceutical Sciences, Center for Biomolecular Sciences, College of Pharmacy, University of Illinois at Chicago, Chicago, Illinois 60612, United States*

Manead Khin − *Department of Pharmaceutical Sciences, Center for Biomolecular Sciences, College of Pharmacy, University of Illinois at Chicago, Chicago, Illinois 60612, United States;* orcid.org/0000-0002-5744-9584

Gauri Shetye − *Institute for Tuberculosis Research, College of Pharmacy, University of Illinois at Chicago, Chicago, Illinois 60612, United States*

Duc Nguyen − *Institute for Tuberculosis Research, College of Pharmacy, University of Illinois at Chicago, Chicago, Illinois 60612, United States*

Mallique Qader − *Institute for Tuberculosis Research, College of Pharmacy, University of Illinois at Chicago, Chicago, Illinois 60612, United States*

https://doi.org/10.1021/acsomega.4c07459
ACS Omega 2024, 9, 44749−44759

Angela C. Nugent − *Institute for Tuberculosis Research, College of Pharmacy, University of Illinois at Chicago, Chicago, Illinois 60612, United States*
Enock Mpofu − *Institute for Tuberculosis Research, College of Pharmacy, University of Illinois at Chicago, Chicago, Illinois 60612, United States*
Camarria Williams − *Boys and Girls Clubs of Chicago, Chicago, Illinois 60612, United States*
Jonathon Rodriguez − *Boys and Girls Clubs of Chicago, Chicago, Illinois 60612, United States*
Joanna E. Burdette − *Department of Pharmaceutical Sciences, Center for Biomolecular Sciences, College of Pharmacy, University of Illinois at Chicago, Chicago, Illinois 60612, United States;* orcid.org/0000-0002-7271-6847
Sanghyun Cho − *Department of Pharmaceutical Sciences, Center for Biomolecular Sciences, College of Pharmacy, University of Illinois at Chicago, Chicago, Illinois 60612, United States; Institute for Tuberculosis Research, College of Pharmacy, University of Illinois at Chicago, Chicago, Illinois 60612, United States;* orcid.org/0000-0003-0926-6246
Scott G. Franzblau − *Department of Pharmaceutical Sciences, Center for Biomolecular Sciences, College of Pharmacy, University of Illinois at Chicago, Chicago, Illinois 60612, United States; Institute for Tuberculosis Research, College of Pharmacy, University of Illinois at Chicago, Chicago, Illinois 60612, United States;* orcid.org/0000-0002-8698-0243
Alessandra S. Eustáquio − *Department of Pharmaceutical Sciences, Center for Biomolecular Sciences, College of Pharmacy, University of Illinois at Chicago, Chicago, Illinois 60612, United States;* orcid.org/0000-0002-7852-7844
Qibin Zhang − *Center for Translational Biomedical Research, University of North Carolina at Greensboro, Greensboro, North Carolina 27412, United States;* orcid.org/0000-0002-6135-8706

Complete contact information is available at: https://pubs.acs.org/10.1021/acsomega.4c07459

Notes

The authors declare no competing financial interest.

■ ACKNOWLEDGMENTS

The authors would like to acknowledge volunteer outreach mentors Lisa Rusali, Ian McIntire, and Dr. Diandra Taylor of UIC; William Edmondson, Ahmad Qadafi, and Jason Vasquez of the Boys and Girls Clubs of Chicago; Kyle Kremiller and Andrew Riley for assistance with the hydrogenation reaction; Aleksej Krunic for assistance with setting up 2D NMR experiments. Research reported in this publication was supported by the UIC Graduate College, Illinois-Indiana Sea Grant (IISG) award number R/22-1-03, IISG Faculty Scholar Award, and the IISG Graduate Student Scholar Award. OzID-MS experiments were supported by the National Institute of Diabetes and Digestive and Kidney Diseases of the National Institutes of Health under Award No. R01DK123499.

■ REFERENCES

(1) Ruffins, P. The Disconnect between Colleges and Their Communities. *Black Issues Higher Educ.* **2002**, *19*, 16−26.
(2) Lee, J.-H.; Ma, R.; Nguyen, L.; Khan, S.; Qader, M.; Mpofu, E.; Shetye, G.; Krull, N. K.; Augustinović, M.; Omarsdottir, S.; Cho, S.; Franzblau, S. G.; Murphy, B. T. Discovery of a New Antibiotic Demethoxytetronasin Using a Dual-Sided Agar Plate Assay (DAPA). *ACS Infect. Dis.* **2023**, *9* (8), 1593−1601.
(3) Nothias, L.-F.; Petras, D.; Schmid, R.; Dührkop, K.; Rainer, J.; Sarvepalli, A.; Protsyuk, I.; Ernst, M.; Tsugawa, H.; Fleischauer, M.; Aicheler, F.; Aksenov, A. A.; Alka, O.; Allard, P.-M.; Barsch, A.; Cachet, X.; Caraballo-Rodriguez, A. M.; Da Silva, R. R.; Dang, T.; Garg, N.; Gauglitz, J. M.; Gurevich, A.; Isaac, G.; Jarmusch, A. K.; Kameník, Z.; Kang, K. B.; Kessler, N.; Koester, I.; Korf, A.; Le Gouellec, A.; Ludwig, M.; Martin, H. C.; McCall, L.-I.; McSayles, J.; Meyer, S. W.; Mohimani, H.; Morsy, M.; Moyne, O.; Neumann, S.; Neuweger, H.; Nguyen, N. H.; Nothias-Esposito, M.; Paolini, J.; Phelan, V. V.; Pluskal, T.; Quinn, R. A.; Rogers, S.; Shrestha, B.; Tripathi, A.; van der Hooft, J. J. J.; Vargas, F.; Weldon, K. C.; Witting, M.; Yang, H.; Zhang, Z.; Zubeil, F.; Kohlbacher, O.; Böcker, S.; Alexandrov, T.; Bandeira, N.; Wang, M.; Dorrestein, P. C. Feature-Based Molecular Networking in the GNPS Analysis Environment. *Nat. Methods* **2020**, *17* (9), 905−908.
(4) Shannon, P.; Markiel, A.; Ozier, O.; Baliga, N. S.; Wang, J. T.; Ramage, D.; Amin, N.; Schwikowski, B.; Ideker, T. Cytoscape: A Software Environment for Integrated Models of Biomolecular Interaction Networks. *Genome Res.* **2003**, *13* (11), 2498−2504.
(5) Wang, M.; Carver, J. J.; Phelan, V. V.; Sanchez, L. M.; Garg, N.; Peng, Y.; Nguyen, D. D.; Watrous, J.; Kapono, C. A.; Luzzatto-Knaan, T.; Porto, C.; Bouslimani, A.; Melnik, A. V.; Meehan, M. J.; Liu, W.-T.; Crüsemann, M.; Boudreau, P. D.; Esquenazi, E.; Sandoval-Calderón, M.; Kersten, R. D.; Pace, L. A.; Quinn, R. A.; Duncan, K. R.; Hsu, C.-C.; Floros, D. J.; Gavilan, R. G.; Kleigrewe, K.; Northen, T.; Dutton, R. J.; Parrot, D.; Carlson, E. E.; Aigle, B.; Michelsen, C. F.; Jelsbak, L.; Sohlenkamp, C.; Pevzner, P.; Edlund, A.; McLean, J.; Piel, J.; Murphy, B. T.; Gerwick, L.; Liaw, C.-C.; Yang, Y.-L.; Humpf, H.-U.; Maansson, M.; Keyzers, R. A.; Sims, A. C.; Johnson, A. R.; Sidebottom, A. M.; Sedio, B. E.; Klitgaard, A.; Larson, C. B.; Boya P, C. A.; Torres-Mendoza, D.; Gonzalez, D. J.; Silva, D. B.; Marques, L. M.; Demarque, D. P.; Pociute, E.; O'Neill, E. C.; Briand, E.; Helfrich, E. J. N.; Granatosky, E. A.; Glukhov, E.; Ryffel, F.; Houson, H.; Mohimani, H.; Kharbush, J. J.; Zeng, Y.; Vorholt, J. A.; Kurita, K. L.; Charusanti, P.; McPhail, K. L.; Nielsen, K. F.; Vuong, L.; Elfeki, M.; Traxler, M. F.; Engene, N.; Koyama, N.; Vining, O. B.; Baric, R.; Silva, R. R.; Mascuch, S. J.; Tomasi, S.; Jenkins, S.; Macherla, V.; Hoffman, T.; Agarwal, V.; Williams, P. G.; Dai, J.; Neupane, R.; Gurr, J.; Rodríguez, A. M. C.; Lamsa, A.; Zhang, C.; Dorrestein, K.; Duggan, B. M.; Almaliti, J.; Allard, P.-M.; Phapale, P.; Nothias, L.-F.; Alexandrov, T.; Litaudon, M.; Wolfender, J.-L.; Kyle, J. E.; Metz, T. O.; Peryea, T.; Nguyen, D.-T.; VanLeer, D.; Shinn, P.; Jadhav, A.; Müller, R.; Waters, K. M.; Shi, W.; Liu, X.; Zhang, L.; Knight, R.; Jensen, P. R.; Palsson, B. Ø.; Pogliano, K.; Linington, R. G.; Gutiérrez, M.; Lopes, N. P.; Gerwick, W. H.; Moore, B. S.; Dorrestein, P. C.; Bandeira, N. Sharing and Community Curation of Mass Spectrometry Data with Global Natural Products Social Molecular Networking. *Nat. Biotechnol.* **2016**, *34* (8), 828−837.
(6) Gross, H.; Stockwell, V. O.; Henkels, M. D.; Nowak-Thompson, B.; Loper, J. E.; Gerwick, W. H. The Genomisotopic Approach: A Systematic Method to Isolate Products of Orphan Biosynthetic Gene Clusters. *Chem. Biol.* **2007**, *14* (1), 53−63.
(7) Bando, Y.; Hou, Y.; Seyfarth, L.; Probst, J.; Götze, S.; Bogacz, M.; Hellmich, U. A.; Stallforth, P.; Mittag, M.; Arndt, H. Total Synthesis and Structure Correction of the Cyclic Lipodepsipeptide Orfamide A. *Chem. - Eur. J.* **2022**, *28* (20), No. e202104417.
(8) Vijayasarathy, S.; Prasad, P.; Fremlin, L. J.; Ratnayake, R.; Salim, A. A.; Khalil, Z.; Capon, R. J. C_3 and 2D C_3 Marfey's Methods for Amino Acid Analysis in Natural Products. *J. Nat. Prod.* **2016**, *79* (2), 421−427.
(9) Knowles, S. L.; Vu, N.; Todd, D. A.; Raja, H. A.; Rokas, A.; Zhang, Q.; Oberlies, N. H. Orthogonal Method for Double-Bond Placement via Ozone-Induced Dissociation Mass Spectrometry (OzID-MS). *J. Nat. Prod.* **2019**, *82* (12), 3421−3431.
(10) Vu, N.; Brown, J.; Giles, K.; Zhang, Q. Ozone-induced Dissociation on a Traveling Wave High-resolution Mass Spectrometer for Determination of Double-bond Position in Lipids. *Rapid Commun. Mass Spectrom.* **2017**, *31* (17), 1415−1423.

(11) Barrientos, R. C.; Zhang, Q. Fragmentation Behavior and Gas-Phase Structures of Cationized Glycosphingolipids in Ozone-Induced Dissociation Mass Spectrometry. *J. Am. Soc. Mass Spectrom.* **2019**, *30* (9), 1609−1620.
(12) Criegee, R. Mechanism of Ozonolysis. *Angew. Chem., Int. Ed.* **1975**, *14* (11), 745−752.
(13) Brown, S. H. J.; Mitchell, T. W.; Blanksby, S. J. Analysis of Unsaturated Lipids by Ozone-Induced Dissociation. *Biochim. Biophys. Acta, Mol. Cell Biol. Lipids* **2011**, *1811* (11), 807−817.
(14) Aiyar, P.; Schaeme, D.; García-Altares, M.; Flores, D. C.; Dathe, H.; Hertweck, C.; Sasso, S.; Mittag, M. Antagonistic Bacteria Disrupt Calcium Homeostasis and Immobilize Algal Cells. *Nat. Commun.* **2017**, *8* (1), No. 1756.
(15) Frost, D. J.; Gunstone, F. D. The PMR Analysis of Non-Conjugated Alkenoic and Alkynoic Acids and Esters. *Chem. Phys. Lipids* **1975**, *15* (1), 53−85.
(16) Santalova, E. A.; Denisenko, V. A. Analysis of the Configuration of an Isolated Double Bond in Some Lipids by Selective Homonuclear Decoupling. *Nat. Prod. Commun.* **2017**, *12* (12), 1913−1916.
(17) Gunstone, F. D.; Pollard, M. R.; Scrimgeour, C. M.; Vedanayagam, H. S. 13C Nuclear Magnetic Resonance Studies of Olefinic Fatty Acids and Esters. *Chem. Phys. Lipids* **1977**, *18* (1), 115−129.
(18) Fu, X.; Xu, Z.; Gawaz, M.; Lämmerhofer, M. UHPLC-MS/MS Method for Chiral Separation of 3-Hydroxy Fatty Acids on Amylose-Based Chiral Stationary Phase and Its Application for the Enantioselective Analysis in Plasma and Platelets. *J. Pharm. Biomed. Anal.* **2023**, *223*, No. 115151.
(19) De Roo, V.; Verleysen, Y.; Kovács, B.; De Vleeschouwer, M.; Muangkaew, P.; Girard, L.; Höfte, M.; De Mot, R.; Madder, A.; Geudens, N.; Martins, J. C. An Nuclear Magnetic Resonance Fingerprint Matching Approach for the Identification and Structural Re-Evaluation of Pseudomonas Lipopeptides. *Microbiol. Spectrum* **2022**, *10* (4), No. e0126122.
(20) Geudens, N.; Martins, J. C. Cyclic Lipodepsipeptides From *Pseudomonas* spp. − Biological Swiss-Army Knives. *Front. Microbiol.* **2018**, *9*, No. 1867.
(21) Clark, C. M.; Costa, M. S.; Conley, E.; Li, E.; Sanchez, L. M.; Murphy, B. T. Using the Open-Source MALDI TOF-MS IDBac Pipeline for Analysis of Microbial Protein and Specialized Metabolite Data. *J. Visualized Exp.* **2020**, No. 147.
(22) Costa, M. S.; Clark, C. M.; Ómarsdóttir, S.; Sanchez, L. M.; Murphy, B. T. Minimizing Taxonomic and Natural Product Redundancy in Microbial Libraries Using MALDI-TOF MS and the Bioinformatics Pipeline IDBac. *J. Nat. Prod.* **2019**, *82* (8), 2167−2173.
(23) Wick, R. R.; Judd, L. M.; Gorrie, C. L.; Holt, K. E. Unicycler: Resolving Bacterial Genome Assemblies from Short and Long Sequencing Reads. *PLoS Comput. Biol.* **2017**, *13* (6), No. e1005595.
(24) Meier-Kolthoff, J. P.; Göker, M. TYGS Is an Automated High-Throughput Platform for State-of-the-Art Genome-Based Taxonomy. *Nat. Commun.* **2019**, *10* (1), No. 2182.
(25) Blin, K.; Shaw, S.; Augustijn, H. E.; Reitz, Z. L.; Biermann, F.; Alanjary, M.; Fetter, A.; Terlouw, B. R.; Metcalf, W. W.; Helfrich, E. J. N.; van Wezel, G. P.; Medema, M. H.; Weber, T. antiSMASH 7.0: New and Improved Predictions for Detection, Regulation, Chemical Structures and Visualisation. *Nucleic Acids Res.* **2023**, *51* (W1), W46−W50.
(26) Hudzicki, J. Kirby-Bauer Disk Diffusion Susceptibility Test Protocol. *Am. Soc. Microbiol.* **2009**, 1−23.
(27) Wishart, D. S.; Sayeeda, Z.; Budinski, Z.; Guo, A.; Lee, B. L.; Berjanskii, M.; Rout, M.; Peters, H.; Dizon, R.; Mah, R.; Torres-Calzada, C.; Hiebert-Giesbrecht, M.; Varshavi, D.; Varshavi, D.; Oler, E.; Allen, D.; Cao, X.; Gautam, V.; Maras, A.; Poynton, E. F.; Tavangar, P.; Yang, V.; van Santen, J. A.; Ghosh, R.; Sarma, S.; Knutson, E.; Sullivan, V.; Jystad, A. M.; Renslow, R.; Sumner, L. W.; Linington, R. G.; Cort, J. R. NP-MRD: The Natural Products Magnetic Resonance Database. *Nucleic Acids Res.* **2022**, *50* (D1), D665−D677.
(28) Hou, Y.; Bando, Y.; Flores, D. C.; Hotter, V.; Das, R.; Schiweck, B.; Melzer, T.; Arndt, H.; Mittag, M. A Cyclic Lipopeptide Produced by an Antagonistic Bacterium Relies on its Tail and Transient Receptor Potential-type Ca^{2+} Channels to Immobilize a Green Alga. *New Phytol.* **2023**, *237*, 1620−1635.
(29) Jang, J. Y.; Yang, S. Y.; Kim, Y. C.; Lee, C. W.; Park, M. S.; Kim, J. C.; Kim, I. S. Identification of Orfamide A as an Insecticidal Metabolite Produced by *Pseudomonas protegens* F6. *J. Agric. Food Chem.* **2013**, *61*, 6786−6791.

https://doi.org/10.1021/acsomega.4c07459
ACS Omega 2024, 9, 44749−44759